Novel Approach to Optically Active Enone–Iron Carbonyl Complexes. Correlation between Their Absolute Configuration and Circular Dichroism

Bruce R. Bender, Markus Koller, Anthony Linden, Alessandro Marcuzzi, and Wolfgang von Philipsborn*

Organisch-chemisches Institut, Universität Zürich, Winterthurerstrasse 190, CH-8057 Zürich, Switzerland

Received June 23, 1992

Enantiomerically enriched (η^4-benzylideneacetone)$Fe(CO)_2(L)$ complexes (L = trimethoxyphosphine, tributylphosphine) have been obtained by decarbonylation of racemic (η^2-benzylideneacetone)$Fe(CO)_3(L)$ with brucine *N*-oxide as the decarbonylating agent. Single-crystal X-ray diffraction has been used to confirm the absolute configuration of (*pR*)-[$Fe(CO)_2((MeO)_3P)$((*E*)-4-phenylbut-3-en-2-one)] ((−)-**3**) and (*pR*)-[$Fe(CO)_2((Bu_3P)$((*E*)-4-phenylbut-3-en-2-one)] ((−)-**7**). (−)-**3** crystallized in the orthorhombic space group $P2_12_12_1$ with a = 15.165 (1) Å, b = 15.558 (2) Å, c = 7.174 (2) Å, and Z = 4, and (−)-**7** crystallized in the same space group with a = 12.036 (1) Å, b = 24.087 (2) Å, c = 8.609 (1) Å, and Z = 4. Several other enantiomerically enriched compounds of this type have been obtained by the same method. Moreover, four configurationally pure (η^4-enone)$Ru(CO)_2(L)$ complexes have been prepared either by use of a chiral enone or by substitution via an optically active phosphine. Circular dichroism (CD) spectra of the complexes have been measured, and a general rule for predicting the absolute configuration of (η^4-enone)$Fe(CO)_2(L)$ and (η^4-enone)$Ru(CO)_2(L)$ complexes is presented.

Introduction

Many optically active (η^4-diene)iron carbonyl complexes have been prepared and reported in the literature.[1] In most cases, they have been obtained by classical resolution methods such as separation of diastereomeric derivatives. Other methods have successfully resolved racemic mixtures with good results including stereoselective decomposition with circularly polarized light,[1b] HPLC separation using a chiral column,[1c] kinetic resolution via stereoselective allylboration,[1d] and enzymatic hydrolysis of racemic ester complexes.[1e]

Surprisingly, fewer reported examples of optically active (η^4-enone)iron carbonyl complexes appear in the literature,[2] even though such complexes have proved to be much more versatile and synthetically useful sources of the $Fe(CO)_3$ moiety. These complexes, which behave as optically active transfer reagents,[2b] have also been obtained via classical methods such as complexation with chiral enone ligands, e.g. (+)-pulegone and (+)-pinocarvone followed by separation of the diastereomers.[2a-c] Diastereocontrolled $Fe(CO)_3$ complexation of a simple heterodiene via an adjacent $Cr(CO)_3$-bearing chiral center has also been reported.[2d] We have recently obtained (η^4-benzylideneacetone)$Fe(CO)_3$ (**1**) highly enriched in one enantiomer by first treating racemic **1** with 1 equiv of (+)-neomenthyldiphenylphosphine, (+)-NMDPP, separating the diastereomers, and then treating a single diastereomer with CO to re-form the tricarbonyl complex.[3] Here we present a novel stereoselective decarbonylation of (η^2-enone)$Fe(CO)_3(L)$ complexes (L = phosphines, phosphites) using a chiral amine oxide

Scheme I. Enantioselective Decarbonylation of η^2-Enone Complexes with Brucine *N*-Oxide

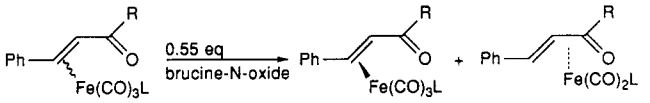

	R	L		
2	Me	$P(OMe)_3$	**2**	**3**
4	Me	PMe_2Ph	**4**	**5**
6	Me	PBu_3	**6**	**7**
8	Ph	$P(OMe)_3$	**8**	**9**

which has enabled us to prepare and characterize several optically active (η^4-enone)$Fe(CO)_2(L)$ complexes.

Trimethylamine oxide (TMNO) readily decarbonylates transition-metal carbonyl complexes under relatively mild conditions.[4] Furthermore, Birch and Kelly have already shown that TMNO reacts with (η^4-cyclohexa-1,3-diene)-$Fe(CO)_3$ complexes in the presence of phosphines to give the corresponding (η^4-cyclohexa-1,3-diene)$Fe(CO)_2(L)$ complexes,[5] and we have used this approach to prepare a variety of acyclic (η^4-diene)$M(CO)_2(L)$ (M = Fe, Ru) and (η^4-enone)$Fe(CO)_2(L)$ complexes.[6]

The mechanism of TMNO induced decarbonylation appears to involve nucleophilic attack at a coordinated CO by the N-oxygen, followed by an irreversible fragmentation to form CO_2 with the amine initially remaining in the metal coordination sphere.[7] Basolo and co-workers[8] have studied the kinetics of the reaction for a variety of metal carbonyls and amine oxides, and the rate law is first order in both amine oxide and metal carbonyl complex, indicative of an associative mechanism. It seemed plausible that a chiral

(1) (a) For a review of chiral acyclic (η^4-diene)$Fe(CO)_3$ complexes, see: Greé, R. *Synthesis* **1989**, 341. (b) Litman, S.; Gedanken, A.; Goldschmidt, Z.; Bakal, Y. *J. Chem. Soc., Chem. Commun.* **1978**, 983. (c) Tajiri, A.; Morita, N.; Asao, T.; Hatano, M. *Angew. Chem.* **1985**, *97*, 342. (d) Roush, W. R.; Park, J. C. *Tetrahedron Lett.* **1990**, *31*, 4707. (e) Alcock, N. W.; Crout, D. H. G.; Henderson, C. M.; Thomas, S. E. *J. Chem. Soc., Chem. Commun.* **1988**, 746.

(2) (a) Koerner von Gustorf, E.; Grevels, F. W.; Krüger, C.; Olbrich, G.; Mark, F.; Schulz, D.; Wagner, R. *Z. Naturforsch., B: Anorg. Chem., Org. Chem.* **1972**, *27*, 392. (b) Birch, A. J.; Raverty, W. D.; Stephenson, G. R. *Tetrahedron Lett.* **1980**, *21*, 197. (c) Birch, A. J.; Raverty, W. D.; Stephenson, G. R. *Organometallics* **1984**, *3*, 1075. (d) Mahmoudi, M. A.; Lamiot, J. C.; Baert, F.; Maciejewski, L. A.; Brocard, J. S. *J. Chem. Soc., Chem. Commun.* **1990**, 1051.

(3) Marcuzzi, A.; Linden, A.; Rentsch, D.; von Philipsborn, W. *J. Organomet. Chem.* **1992**, 429, 87.

(4) Albers, M. O.; Coville, N. *J. Coord. Chem. Rev.* **1984**, *53*, 227.

(5) Birch, A. J.; Kelly, L. F. *J. Organomet. Chem.* **1985**, *286*, C5.

(6) Adams, C. M.; Hafner, A.; Koller, M.; Marcuzzi, A.; Prewo, R.; Solana, I.; Vincent, B.; von Phillipsborn, W. *Helv. Chim. Acta* **1989**, *72*, 1658.

(7) Collman, J. P.; Hegedus, L. S.; Norton, J. R.; Finke, R. G. *Principles and Applications of Organotransition Metal Chemistry*, 2nd ed.; University Science Books,: Mill Valley, CA, 1987; p 264.

(8) (a) See: Shen, J.-K.; Gao, Y.-C.; Shi, Q.-Z.; Basolo, F. *J. Organomet. Chem.* **1991**, *401*, 295 and references cited therein. (b) Gao, Y.-C.; Shi, Q.-Z.; Kershner, D. L.; Basolo, F. *Inorg. Chem.* **1988**, *27*, 188. (c) Shen, J.-K.; Gao, Y.-C.; Shi, Q.-Z.; Rheingold, A. L.; Basolo, F. *Inorg. Chem.* **1991**, *30*. 1868.

0276-7333/92/2311-4268$03.00/0 © 1992 American Chemical Society

Table I. Enantioselective Decarbonylation of η^2-Enone Complexes with Brucine *N*-Oxide in THF

complex	reacn temp, deg	reacn time, h	yield, %	ee, %
2	−10	3	45	
3			49	49
4	−10	6	43	
5			41	84
6	0	4	46	
7			43	66
8	0	2	42	
9			50	27

Scheme II. Enantioselective CO Displacement of Tricarbonyl[0–4-η-((*E*)-4-phenylbut-3-en-2-one)]iron (1)

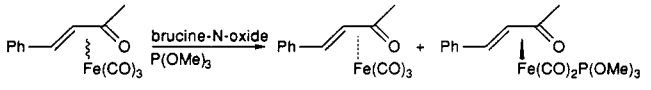

1 **1** (15% ee) **3** (15% ee)

amine oxide might react preferentially with one enantiomer of a racemic mixture of an (η^2-enone)iron carbonyl complex (Scheme I). Such kinetic resolution has already been demonstrated by Roush and co-workers in the case of the resolution of racemic (η^4-diene)$Fe(CO)_3$ complexes using stereoselective allylboration.[1d]

We also describe here the circular dichroism (CD) spectra of optically active (η^4-enone)$M(CO)_2(L)$ (M = Fe, Ru) complexes. The optical properties of these complexes are due to planar chirality which arises from metal complexation of the two enantiotopic faces of the heterodiene. Knowledge of the absolute configuration of optically active ene– and diene–metal complexes often allows the prediction of the configuration of newly created chiral centers, due to the strong stereodirecting effect of the metal.

We have already suggested that there could be a direct correlation between the sign of the Cotton effect of these complexes and their absolute configuration.[3] We now have been able to confirm this hypothesis by the synthesis of several optically active complexes, determining their absolute configuration by X-ray structure analyses, and comparing the results with their CD spectra.

Results

1. Enantioselective Decarbonylation of η^2-Complexes. Amine oxides are readily prepared from the corresponding tertiary amines. The amino group is oxidized by either hydrogen peroxide or 2-(phenylsulfonyl)-3-phenyloxaziridine (Davis' reagent), which reacts with amines that are more basic than pyridine.[9] Different chiral amine oxides such as (−)-*N*-methylephedrine *N*-oxide and quinine *N*-oxide were tested. Brucine *N*-oxide has proven to give the highest enantiomeric excess (ee) values (Table I) and the best reproducibility in the decarbonylation reaction (Scheme I). In every case, the product of the apparent kinetic resolution was richer in one enantiomer of **3**, **5**, **7**, and **9**, all of which had negative $[\alpha]_D$ values. The product solutions also contained unreacted **2**, **4**, **6**, and **8**, all of which had positive $[\alpha]_D$ values. Separation was achieved by column chromatography.

On the other hand, direct displacement of one CO of racemic **1** by brucine *N*-oxide at −60 °C in the presence of trimethoxyphosphine followed by quenching of the reaction after 4 h yielded the corresponding enantiomerically inversely enriched **3** ((+)-**3**/(−)-**3** = 4:3), which was isolated

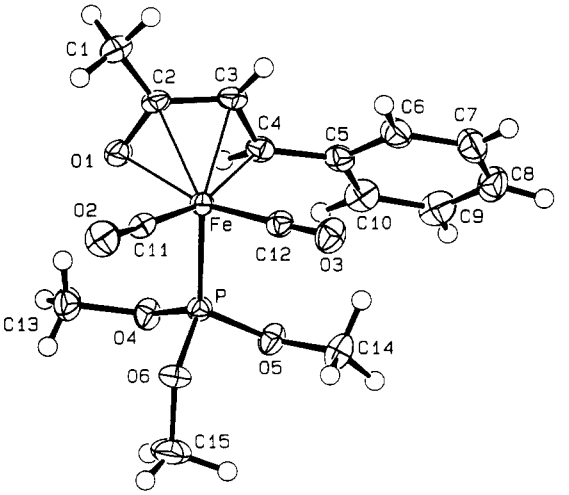

Figure 1. Molecular structure of (*pR*)-[$Fe(CO)_2$(($MeO)_3$P)-((*E*)-4-phenylbut-3-en-2-one)] ((−)-**3**).

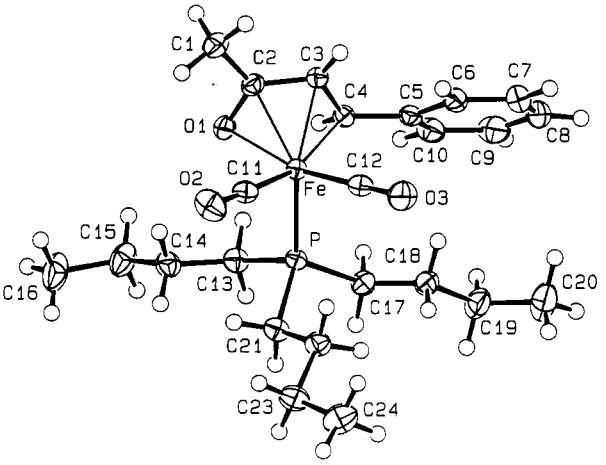

Figure 2. Molecular structure of (*pR*)-[$Fe(CO)_2$(Bu_3P)((*E*)-4-phenylbut-3-en-2-one)] ((−)-**7**).

in 41% yield, whereas the starting material ((+)-**1**/(−)-**1** = 3:4) was recovered in 44% yield (Scheme II).

2. Crystal Structure and Absolute Configuration of (−)-3 and (−)-7. X-ray data were acquired on red-orange crystals of (−)-**3** and (−)-**7** respectively. The crystal data and refinement details are listed in Table III. The refinement and tests for absolute configuration yielded the structures with the *pR* configuration shown in Figures 1 and 2. The absolute configuration was determined by two methods. The first method involved refining the structure to convergence (R = 0.0239, R_w = 0.0247 for (−)-**3**; R = 0.0273, R_w = 0.0244 for (−)-**7** and then refining the inverted atomic coordinates with the identical set of refinable parameters and reflections (R = 0.0401, R_w = 0.0434 for (−)-**3**; R = 0.0417, R_w = 0.0404 for (−)-**7**). The Hamilton R-factor ratio test[10] showed that at 3σ confidence limits the refinements were significantly different and that the initially refined enantiomorph was the correct one. The second method involved the use of Flack's x parameter[11] to determine the fractional contribution of each enantiomorph to the observed data. This is a refinable parameter which describes the structure as an inversion twin and indicates the fraction of the inverse structure, x, in the sample. A value of zero indicates that the enantiomorph whose coordinates are used in the refinement is the correct one,

(9) Zajac, W. W.; Jr.; Walters, T. R.; Darcy, M. G. *J. Org. Chem.* **1988**, *53*, 5856.

(10) Hamilton, W. C. *Acta Crystallogr.* **1965**, 18, 502.

(11) (a) Flack, H. D. *Acta Crystallogr., Sect. A* **1983**, *39*, 876. (b) Bernardinelli, G.; Flack, H. D. *Acta Crystallogr., Sect. A* **1985**, *41*, 500.

Chart I

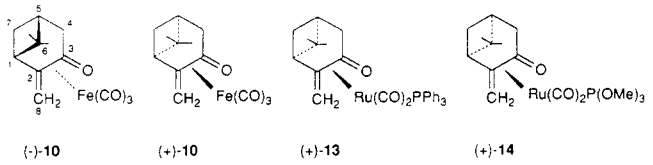

(-)-10 (+)-10 (+)-13 (+)-14

Scheme III

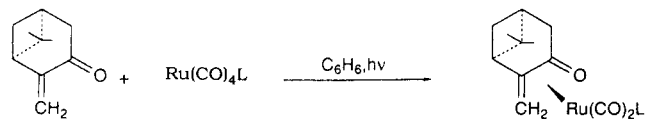

11: L=P(OMe)$_3$
12: L=PPh$_3$

(+)-**13**: L=P(OMe)$_3$
(+)-**14**: L=PPh$_3$

while a value of one would indicate that the inverse enantiomorph is correct. The reflection data and atomic coordinates, which had been refined using TEXSAN,[12] were transferred to CRYSTALS[13] in which it is possible to refine the enantiopole, or Flack's x, parameter. After initial refinement of the structure to convergence, the enantiopole parameter was also refined and converged to a value of 0.01 (1) and 0.00 (1) for (−)-**3** and (−)-**7**, respectively, which confidently confirms that the refined coordinates represent the true enantiomorph.

Fractional atomic coordinates and equivalent isotropic temperature factors are listed in Table IV. Selected bond lengths and angles are summarized in Table V. The anisotropic thermal parameters and structure factors are given in the supplementary material. In both cases, the coordination geometry of the Fe atom may be described as a distorted square pyramid with the phosphine ligand in the apical position and is essentially the same as in **1** and related compounds.[6]

3. Synthesis of Other Enantiomerically Pure η^4-Heterodiene Complexes. (−)-(η^4-pinocarvone)Fe(CO)$_3$, (−)-**10**, and (+)-(η^4-pinocarvone)Fe(CO)$_3$, (+)-**10**, were synthesized from (+)- and (−)-pinocarvone, respectively, according to the procedure of Koerner von Gustorf et al.[2a] They had shown that, upon complexation of pinocarvone with Fe(CO)$_5$, only one of the two possible diastereomers was formed. Their X-ray study showed that the Fe(CO)$_3$ moiety is attached to the side opposite to the methyl groups of the bridge (Chart I).

The two ruthenium complexes (+)-(η^4-pinocarvone)Ru(CO)$_2$(P(OMe)$_3$), (+)-**13**, and (+)-η^4-pinocarvone)Ru(CO)$_2$(PPh$_3$), (+)-**14**, were obtained from the reaction of the corresponding mononuclear ruthenium complexes Ru(CO)$_4$P(OMe)$_3$, **11**, and Ru(CO)$_4$PPh$_3$, **12**, with the chiral ligand (−)-pinocarvone[14] (Scheme III).

In accordance with other reported examples,[2a,15] we presume that the coordination site in these complexes is also opposite to the methyl groups of the bridge. In each case only one diastereomer could be detected in the ^{1}H- and ^{31}P-NMR spectra. Yields for these two latter reactions ranged from 40 to 50%, and the products were isolated as thermally stable yellow oils.

Scheme IV

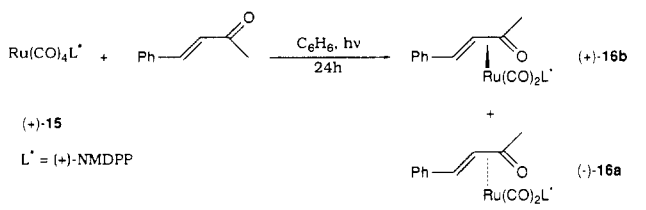

Chart II

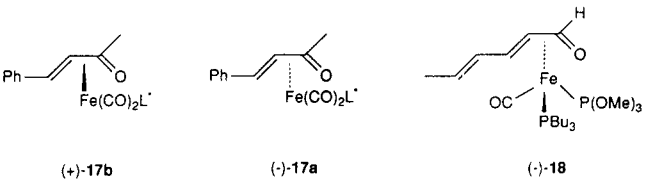

(+)-**17b** (-)-**17a** (-)-**18**

L* = (+)-NMDPP

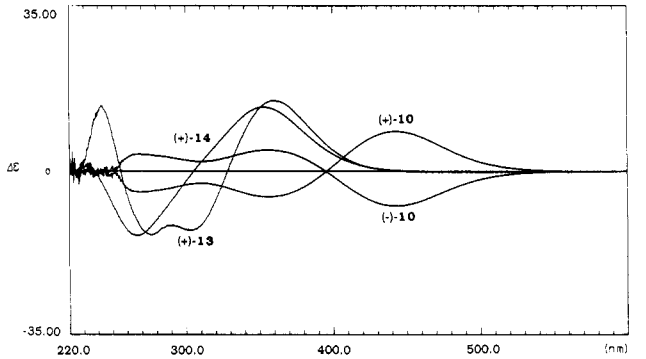

Figure 3. CD spectra of (η^4-pinocarvone)iron and -ruthenium complexes.

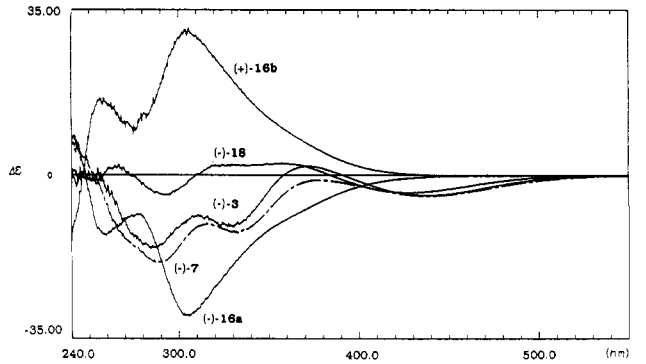

Figure 4. CD spectra of (η^4-enone)iron and -ruthenium complexes.

Two additional enantiomerically pure ruthenium complexes of benzylideneacetone were synthesized by the same method: Ru(CO)$_4$L* (L* = (+)-neomenthyldiphenylphosphine, (+)-NMDPP, (+)-**15**) reacted with the organic ligand to give two diastereomers (−)-**16a** and (+)-**16b**, which could easily be separated by column chromatography. The two products could be isolated in a yield of 65% (ratio approximately 1:1) (Scheme IV).

Another three enantiomerically pure complexes that we have used to test our CD rule were recently described by our group.[3,16] (−)-(η^4-benzylideneacetone)Fe(CO)$_2$((+)-NMDPP), (−)-**17a**, and (+)-(η^4-benzylideneacetone)Fe(CO)$_2$((+)-NMDPP), (+)-**17b**, were prepared by treating (*rac*)-**1** with (+)-NMDPP. The third complex (−)-**18** was obtained as a side product during our earlier studies[16] (Chart II).

(12) TEXSAN-TEXRAY Single Crystal Structure Analysis Package, Version 5.0. Molecular Structure Corp., The Woodlands, TX, 1989.
(13) Carruthers, J. R.; Watkin, D. L. CRYSTALS, Issue 9, Chemical Crystallography Laboratory, Oxford, U.K., 1986.
(14) These two mononuclear Ru complexes were synthesized by irradiation of a hexane solution of Ru$_3$(CO)$_{12}$ with an excess of phosphine ligand. For characterization, see: (a) L'Eplattenier, F.; Calderazzo, F. *Inorg. Chem.* **1968**, *7*, 1290. (b) Cobbledick, R. E.; Einstein, F. W. B.; Pomeroy, R. K.; Spetch, E. R. *J. Organomet. Chem.* **1980**, *195*, 77.
(15) Salzer, A.; Schmalle, H.; Stauber, R.; Streiff, S. *J. Organomet. Chem.* **1991**, *408*, 403.
(16) Rentsch, D. Diploma Thesis, University of Zurich, 1991.

Table II. Chiroptical Data

complex	$[\alpha_0]_D$ (CH_2Cl_2) (c g/100 mL)	λ_1, nm (ΔE_1, M^{-1} cm^{-1})	λ_2, nm (ΔE_2, M^{-1} cm^{-1})	λ_3, nm (ΔE_3, M^{-1} cm^{-1})	λ_4, nm (ΔE_4, M^{-1} cm^{-1})
(-)-3	-1056 (0.300) -1012[a] -1056[b]	436.8 (-4.45)	373.6 (1.88)	330.0 (-11.14)	284.4 (-15.80)
(-)-5	-1336[c]				
(-)-7	-1152 (0.262)	441.2 (-4.59)	377.6 (-1.07)	332.8 (-12.46)	287.6 (-18.77)
(-)-9	-1275[d]				
(+)-10	+1338 (0.540)	442.8 (8.47)	356.4 (-5.47)	312.0 (-2.55)	268.4 (-4.51)
(+)-13	+379 (0.210)	360.0 (15.00)	300.8 (-12.66)	290.4 (-11.47)	276.4 (-13.64)
(+)-14	+484 (0.240)	353.2 (13.62)	268.0 (-13.79)		
(-)-16a	-693 (0.167)	305.2 (-30.11)	278.8 (-8.34)	259.6 (-13.11)	241.2 (8.41)
(+)-16b	+718 (0.313)	305.6 (31.13)	274.8 (8.60)	258.4 (16.29)	238.8 (-17.43)
(-)-17a	-1066 (0.155)	344.0 (-8.22)	323.2 (-6.13)	294.0 (-17.23)	248.8 (14.31)
(+)-17b	+1166 (0.155)	346.0 (11.00)	325.0 (8.55)	293.6 (17.27)	250.0 (-11.19)
(-)-18	-317 (0.195)	427.0 (-3.65)	358.0 (2.42)	292.0 (-4.09)	

[a] Determined via direct CO displacement of enriched 1 ((-)-1/(+)-1 = 4:1)[3] with known $[\alpha_0]_D$. [b] Calculated from ^1H NMR (300 MHz, C_6D_6) shift experiment with addition of 0.2 equiv of Eu(tfc)$_3$. [c] Determined via direct CO displacement of enriched 1 ((-)-1/(+)-1 = 5:1)[3] with known $[\alpha_0]_D$. [d] Calculated from ^{31}P NMR (80.7 MHz, C_6D_6) shift experiment with addition of 1 equiv of Eu(tfc)$_3$.

The planar chirality of (+)-**17b** has been determined by X-ray analysis and has been described together with its CD spectrum in a previous paper.[3] The complex (-)-**18** was formed from (η^4-(2*E*,4*E*)-hexa-2,4-dienal)Fe(CO)$_3$ of known absolute configuration. Because the replacement of iron by ruthenium has no influence on either the sign of the Cotton effect or the sign of $[\alpha_0]_D$, and since the absolute configuration of the (+)-NMDPP group is the same as in (+)-**17b**, the chiroptic evidence leads to the *pS* chirality also for (+)-**16b**.

4. Circular Dichroism Data. All CD spectra were measured between 200 and 600 nm. Methanol was used as solvent, and the data were collected at ambient temperature. The spectra of the complexes prepared from (-)- and (+)-pinocarvone appear in Figure 3, whereas the spectra of the acyclic compounds are shown in Figure 4. Chiroptical data are listed in Table II. Although there are small shifts in the position of the maxima, all complexes (except (+)-**10** and (-)-**10**) show their most intense band between 280 and 350 nm. The ruthenium complexes have significantly smaller $[\alpha]_D$ values and more intense CD maxima than the iron analogues ((-)-**16a**/(+)-**16b** vs (-)-**17a**/(+)-**17b**). The chiral phosphine (+)-NMDPP does not have a great influence on the CD spectra of such planar chiral substances, since the CD spectra of the diastereomeric pair (-)-**16a**/(+)-**16b** (both of which contain (+)-NMDPP) look like mirror images. This is in agreement with earlier observations.[3,17] On the other hand, η^4-heterodiene carbonyl complexes which have opposite planar chirality show Cotton effects with different signs, in agreement with previous studies of η^4-diene carbonyl complexes.[18] Just as in other transition-metal derivatives,[1c,e,18,19a] we found that the sign of the Cotton effect at long wavelengths (d-d transition) can be correlated with their absolute configuration.

Discussion

Brucine, a chiral tertiary amine, has previously been used to resolve racemic Fe(CO)$_4$(η^2-olefin) complexes of acrylic and fumaric acid,[19] while trimethylamine *N*-oxide (TMNO) has been extensively used as a decarbonylation reagent for metal-carbonyl complexes.[4] We have combined aspects of both reagents in the form of a chiral tertiary amine oxide. By analogy to the thermally induced loss of one CO from (η^2-enone)Fe(CO)$_3$(L) (L = CO, phosphine), which has previously been shown to give the corresponding (η^4-enone)Fe(CO)$_2$(L) complexes,[20] we have used brucine *N*-oxide to remove one CO from racemic (η^2-enone)Fe(CO)$_3$(L) complexes. The stereoselectivity observed might arise via a diastereomeric transition state, in which the brucine *N*-oxide preferentially attacks a carbonyl of one enantiomer of the η^2-enone complex. The vacant coordination site may then be irreversibly chelated by the η^2-enone ligand to form a stable η^4-enone product with enantiomeric excess. Interestingly, the direct reaction of **1** with brucine *N*-oxide in the presence of trimethyl phosphite exhibits the opposite enantioselectivity (Scheme II), although with less enantiomeric excess (ee).

PMe_2Ph or PBu_3 in the coordination sphere of iron as in **4** and **6** slows down the nucleophilic attack by brucine *N*-oxide (Table I). We attribute this to electronic factors, as PMe_2Ph and PBu_3 are both better σ-donors than P(OMe)$_3$. The increased electron density at the metal increases the Fe–CO π-back-bonding and renders the CO carbon less susceptible to nucleophilic attack. This is also reflected in the stretching frequency of the highest CO band in the IR (**4**, 2040 cm^{-1}; **6**, 2040 cm^{-1}; **2**, 2060 cm^{-1}; **8**, 2060 cm^{-1}; in CH_2Cl_2) and is in agreement with rate studies of CO oxidation by TMNO of Mo(CO)$_5$L complexes as a function of the electron-donor properties of the ligand L.[8b] The same tendency has been observed for the thermal loss of CO;[20f] complex **2** is decarbonylated in refluxing benzene, whereas **4** is only subject to enone dissociation and exchange under these conditions and thus indicates a more stable Fe–CO bond.

At present we do not understand how the steric properties of (η^2-enone)Fe(CO)$_3$(L) or the brucine *N*-oxide complex might affect the stereoselectivity of the decar-

(17) Howell, J. A. S.; Tirvengadum, M. C.; Squibb, A. D.; Walton, G.; McArdle, P.; Cunningham, D. *J. Organomet. Chem.* **1988**, *347*, C5.

(18) (a) Stephenson, G. R.; Howard, P. W.; Taylor, S. C. *J. Chem. Soc., Chem. Commun.* **1991**, 127. (b) Howell, J. A. S.; Squibb, A. D.; Goldschmidt, Z.; Gottlieb, H. E.; Almadhoun, A.; Goldberg, I. *Organometallics* **1990**, 9, 80. (c) Djedaini, F.; Greé, D.; Martelli, J.; Greé, R.; Leroy, L.; Bolard, J.; Toupet, L. *Tetrahedron Lett.* **1989**, *30*, 3781. (d) Stephenson, G. R.; Alexander, R. P.; Morley, C.; Howard, P. W. *Phil. Trans. R. Soc. London A* **1988**, *326*, 545. (e) Gabioud, R.; Vogel, P. *Helv. Chim. Acta* **1986**, *69*, 865. (f) Gabioud, R.; Vogel, P. *Helv. Chim. Acta* **1986**, *69*, 271. (g) Barras, C.; Roulet, R. *Inorg. Chim. Acta* **1984**, *82*, L1. (h) Reger, D. L. *J. Inorg. Nucl. Chem.* **1977**, *39*, 1095.

(19) (a) Musco, A.; Palumbo, R.; Paiaro, G. *Inorg. Chim. Acta* **1971**, *5*, 157. (b) Paiaro, G.; Palumbo, R. *Gazz. Chim. Ital.* **1967**, *97*, 265. (c) Paiaro, G.; Palumbo, R.; Musco, A.; Panunzi, A. *Tetrahedron Lett.* **1965**, 1067.

(20) (a) Stark, K.; Lancaster, J. E.; Murdoch, H. D.; Weiss, E. *Z. Naturforsch.* **1964**, *19b*, 284. (b) Howell, J. A. S.; Johnson, B. F. G.; Josty, P. L.; Lewis, J. *J. Organomet. Chem.* **1972**, *39*, 329. (c) Brodie, A. M.; Johnson, B. F. G.; Josty, P. L.; Lewis, J. *J. Chem. Soc., Dalton Trans.* **1972**, 2031. (d) Cardaci, G. *J. Am. Chem. Soc.* **1975**, *97*, 1412. (e) Vessieres, A.; Touchard, D.; Dixneuf, P. *J. Organomet. Chem.* **1976**, *118*, 93. (f) Vessieres, A.; Dixneuf, P. *J. Organomet. Chem.* **1976**, *108*, C5.

Chart III

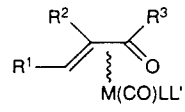

R¹, R², R³: H, alkyl and aryl

L,L' = CO, PR_3 and $P(OR)_3$

bonylation reaction. While the structure of racemic (η^2-benzylideneacetone)$Fe(CO)_3(P(OMe)_3)$, **2**, is known,[21] with the phosphite ligand in an equatorial position, an examination of simple molecular models does not clearly identify any deciding steric factors to rationalize the observed stereoselectivity.

We have observed that solutions enriched in one enantiomer of (η^2-enone)$Fe(CO)_3(L)$ complexes slowly lose their optical activity over time, in contrast to more stable (η^4-enone)$Fe(CO)_2(L)$ products. Assuming that the two enantiomers are in dynamic equilibrium, then perhaps more of the (η^2-enone)$Fe(CO)_3(L)$ molecules could be channeled through the kinetically more favorable pathway. In fact, the yield of optically active **5** can be raised to 90% by running the reaction with 1 equiv of brucine *N*-oxide in benzene at room temperature, giving the product with 34% ee. Raising the temperature to 80 °C improves the ee to 37% but lowers the yield of the reaction (77%).

Another main purpose of this paper is to establish an empirical rule for predicting the absolute configuration of (η^4-enone)$Fe(CO)_2(L)$ complexes from their CD spectra. Such a rule might be useful in the prediction of the absolute configuration of heterodiene complexes of the general formula shown in Chart III.

Both complexes that have been shown by X-ray crystallography to have *pR* configuration; i.e., (−)-**3** and (−)-**7** have negative $[\alpha_0]_D$ values and show a negative Cotton effect at long wavelengths. Both complexes (+)-**17b**[3] and (+)-**10**,[2a] which were previously shown to have a *pS* configuration, have a positive $[\alpha_0]_D$ value and show a positive Cotton effect at long wavelengths. The absorptions at long wavelengths are those that can be correlated with the absolute configuration of the corresponding complexes. The complexes (−)-**10**, (−)-**17a**, and (−)-**18**, which exhibit negative $[\alpha_0]_D$ values and a negative Cotton effect, have the *pR* configuration. Likewise, the complexes (+)-**13** and (+)-**14**, which exhibit positive $[\alpha_0]_D$ values and a positive Cotton effect, have the *pS* configuration. The CD data of **5**, **9**, and the two enantiomeric $Fe(CO)_3$ complexes of (*E*)-4-phenylbut-3-en-2-one ((+)-**1** and (−)-**1**)[3] fit with our rule but are not listed here because the compounds are not enantiomerically pure. The rule also seems to hold for the η^2-complexes **2**, **4**, **6**, and **8**, which are subject to enantiomeric interconversion during the resolution reaction and thus could not be obtained optically pure. Last, it is interesting to note that our results for the prediction of the absolute configuration of (η^4-enone)$Fe(CO)_{3-n}(L)_n$ (n = 1, 2) complexes from their CD spectra agree with similar results reported for optically active (η^4-diene)$Fe(CO)_3$ complexes[18c] and may reflect a general property of the circular dichroism of η^4-heterodiene carbonyl complexes.

Conclusions

We have shown that brucine *N*-oxide oxidizes a carbonyl ligand in racemic (η^2-enone)$Fe(CO)_3(L)$ complexes to form (η^4-enone)$Fe(CO)_2(L)$ complexes with enantiomeric excess. We have determined the absolute configuration of the major product formed in two cases and have correlated the absolute configuration of (η^4-enone)$Fe(CO)_{3-n}(L)_n$ (n = 1, 2) complexes with their CD spectra. We have used this correlation to predict the absolute configuration of several other (η^4-enone)$M(CO)_2(L)$ (M = Fe, Ru) complexes.

Last, with regard to the preparative work reported here, it should be noted that the use of trimethylamine oxide to create a vacant coordination site is a general reaction for transition-metal carbonyl complexes.[4] The use of a chiral amine oxide to stereoselectively remove a carbonyl ligand from a transition-metal carbonyl complex might therefore find use in preparing other optically active transition-metal complexes.

Experimental Section

IR spectra were recorded on a Perkin-Elmer 298 spectrometer. NMR spectra were recorded on Bruker AM-400 and AC-300 and Varian XL-200 spectrometers. δ(H) and δ(C) are reported relative to internal TMS; δ(P) is reported relative to 85% H_3PO_4 as an external standard. The CD spectra were measured on a JASCO J-500A spectrometer. All measurements were made at room temperature, and methanol was used as solvent. All synthetic operations were carried out under inert atmosphere in dry, O_2-free solvents. Chromatographic separations were performed on silica gel 60 (70–230 mesh, Merck). $Ru_3(CO)_{12}$ was purchased from Strem Chemicals and was used without further purification. (+)- and (−)-pinocarvone were synthesized by CrO_3 oxidation of (+)- and (−)-1-*trans*-pinocarveol, which was obtained from the corresponding α-pinene[22] or via direct oxidation of β-pinene with selenium dioxide.[23] The chiral phosphine (+)-NMDPP was synthesized according to the procedure of Morrison et al.[24] Microanalyses of crystalline products gave satisfactory results.

General Procedure for Enanantioselective Decarbonylation. The η^2-complexes **2**, **4**, **6**, and **8** (Scheme I) were synthesized according to literature procedures[20e] and obtained as yellow crystals. A typical decarbonylation reaction was carried out in the following way: the η^2-complex and 0.55 equiv of brucine *N*-oxide were combined in THF at low temperature (see Table I for specific conditions). After 2–6 h the reaction mixture was filtered through a short silica gel column in order to remove the brucine. The η^4-complex and the unreacted η^2-complex were then separated by flash chromatography with hexane/ether as eluent. Specific conditions and results are listed in Table I.

Enantiomerically pure (−)-**3** and (−)-**7** were obtained by several crystallizations of the products of the enantioselective decarbonylation from hexane and their $[\alpha_0]_D$ values measured. Because we could not crystallize pure enantiomers of **5** and **9**, their $[\alpha_0]_D$ values were calculated using either of the two different methods described below. As a cross-check for validity of these methods, the enantiomeric ratio of **3** was also determined by these two methods:

(i) Addition of 0.2 equiv of the chiral NMR shift reagent $Eu(tfc)_3$ effectively separates the signal of the C(3) proton into two broadened signals. A sample of enriched **3** was measured, and the peaks were gravimetrically integrated. The enantiomeric ratio determined by NMR (2:1) was consistent with the enantiomer ratio calculated from $[\alpha_0]_D$; i.e., (−)-**3**/(+)-**3** = 2:1.

(ii) CO displacement of enriched **1** ((−)-**1**/(+)-**1** = 4:1)[3] with trimethoxyphosphine and trimethylamine *N*-oxide[6] gave the corresponding enriched **3** in 81% yield. The $[\alpha]_D$ value was measured, and the enatiomeric ratio (−)-**3**/(+)-**3** was calculated to be 4:1. Comparison of the two extrapolated values with the $[\alpha_0]_D$ value of pure crystalline (−)-**3** (Table II) shows that the shift experiment is reliable and that no racemization occurred during the CO displacement reaction. Because we did not succeed in crystallizing pure enantiomers of **5** and **9**, the $[\alpha_0]_D$ values of (−)-**5** and (−)-**9** were determined from enriched material by analogy to these two methods (Table II).

Tricarbonyl[3,4-η-((*E*)-4-phenylbut-3-en-2-one)](tributylphosphine)iron (6) was synthesized according to literature

(21) Koller, M.; Linden, A.; von Philipsborn, W. Unpublished results.

(22) Schenck, G. O.; Eggert, H.; Denk, W. *Liebigs Ann. Chem.* **1953**, *584*, 177.

(23) (a) Hartshorn, M. P.; Wallis, A. T. A. *J. Chem. Soc.* **1964**, 5254. (b) Stallcup, W. D.; Hawkins, J. E. *J. Am. Chem. Soc.* **1941**, *63*, 3339. (c) Coxon, J. M.; Dansted. E.; Hartshorn, M. P.; Richards, K. E. *Tetrahedron* **1968**, *24*, 1193.

(24) Morrison, J. D.; Masler, W. F. *J. Org. Chem.* **1974**, *39*, 270.

procedures[20e] and recrystallized from hexane in 56% yield, mp 65–67 °C. IR (CH_2Cl_2): 3000–2870, 2040, 1960, 1640 cm^{-1}. ^1H NMR (400 MHz, C_6D_6): δ 7.15–6.90 (m, phenyl H), 4.65 (d, J(HH) = 10.7 Hz, H–C(3)), 3.95 (d, J(HH) = 10.7 Hz, H–C(4)), 2.27 (s, H–C(1)), 1.44–0.80 (m, CH_2), 0.78 (t, J(H,H) = 7.0 Hz, CH_3). ^{31}P NMR (121.5 MHz, acetone-d_6): δ 35.0 (s). MS (EI – mode): m/e 488 (M^+), 460 [$(M - CO)^+$], 432 [$(M - 2CO)^+$], 404 [$(M - 3CO)^+$], 342 [$(M$ – enone$)^+$], 286 [$(M - PBu_3)^+$].

Dicarbonyl[O-4-η-((*E*)-4-phenylbut-3-en-2-one)](tributylphosphine)iron (*rac*-(7)). A 143-mg amount (0.5 mmol) of *rac*-1 was combined with 122 mg (1.1 mmol) of trimethylamine *N*-oxide dihydrate and 222 mg (1.1 mmol) of tributylphosphine in acetonitrile at 0 °C. After 4 h, the reaction mixture was filtered with Et_2O through a short silica gel column. The solvent and excess tributylphosphine were removed in vacuo. A 216-mg amount (94%) of a viscous red oil was isolated. IR (CH_2Cl_2): 3000–2870, 1990, 1930 cm^{-1}. ^1H NMR (300 MHz, C_6D_6): δ 6.97–6.78 (m, phenyl H), 5.14 (dd, J(HH) = 8.2 Hz, J(PH) = 2.1 Hz, H–C(3)), 2.09 (m, H–C(1), H–C(4)), 1.63–0.98 (m, CH_2), 0.60 (t, J(H,H) = 7.0 Hz, CH_3). ^{13}C NMR (50 MHz, acetone-d_6): δ 211.0 (s, CO), 206.3 (s, CO), 143.8 (s, C(2) or phenyl C(1)), 139.0 (s, C(2) or phenyl C(1)), 129.0 (s, phenyl C), 127.3 (s, phenyl C), 125.5 (s, phenyl C), 79.0 (s, C(3)), 57.9 (d, J(PC) = 2 Hz, C(4)), 27.1 (d, J(PC) = 24 Hz, CH_2), 26.1 (s, CH_2), 25.0 (d, J(PC) = 13 Hz, CH_2), 21.5 (s, C(1)), 13.9 (s, CH_3). ^{31}P NMR (80.7 MHz, acetone-d_6): δ 37.8 (s).

(+)-(*pS*)-Dicarbonyl[O-4-η-((–)-pinocarvone)](triphenylphosphine)ruthenium ((+)-13). A mixture of (–)-pinocarvone (1.64 g, 8.42 mmol) and tetracarbonyl(triphenylphosphine)ruthenium (**12**)[14] (0.65 g, 1.36 mmol) in benzene (150 mL) were irradiated with a high-pressure Hg lamp (Philips HPK, 125 W). The reaction mixture was monitored by TLC. After 15 h solvent was removed and the oily residue chromatographed with hexane/Et_2O as eluent yielding 0.35 g (45%) of the desired product as a yellow oil. IR (CH_2Cl_2): 3000–2800, 2010, 1940 cm^{-1}. ^1H NMR (400 MHz, $CDCl_3$): δ 7.49–7.38 (m, phenyl H), 3.18 (m, H–C(4)), 2.82 (ddd, J(HH) = 17.2 Hz, J(HH) = 6.4 Hz, J(PH) = 2.4 Hz, H–C(4)), 2.69 (m, H–C (7-exo)), 2.47 (sept, J(HH) = J(PH) = 2.9 Hz, H–C(5)), 2.29 (t, J(HH) = 5.9 Hz, H–C (7-endo)), 2.01 (d, J(HH) = 9.5 Hz, H–C(1)), 1.64 (t, J(HH) = J(PH) = 1.7 Hz, H–C(8)), 1.45 (s, CH_3), 1.17 (dd, J(PH) = 10.4 Hz, J(HH) = 1.7 Hz, H–C(8)), 1.03 (s, CH_3). ^{13}C NMR (50 MHz, $CDCl_3$): δ 201.1 (d, J(PC) = 9 Hz, CO), 196.5 (s, CO), 139.4 (d, J(PC) = 3 Hz, C(3)), 134.9 (d, J(PC) = 41 Hz, phenyl C(1)), 133.1 (d, J(PC) = 13 Hz, phenyl C(2)), 129.8 (s, phenyl C(4)), 128.2 (d, J(PC) = 10 Hz, phenyl C(3)), 110.1 (d, J(PC) = 2 Hz, C(2)), 43.9 (s, C(1) or C(5)), 42.3 (s, C(5) or C(1)), 39.9 (s, C(6)), 39.8 (d, J(PC) = 5 Hz, C(8)), 36.0 (d, J(PC) = 3 Hz, C(4)), 32.8(d, J(PC) = 2 Hz, C(7)), 27.3 (s, CH_3), 21.7 (s, CH_3). ^{31}P NMR (80.7 MHz, $CDCl_3$): δ 42.2 (s). For optical rotation and CD data, see Table I.

(+)-(*pS*)-Dicarbonyl[O-4-η-((–)-pinocarvone)](trimethyl phosphite)ruthenium ((+)-14). The procedure was the same as for (+)-13. Irradiation time was 26 h. Chromatography yielded 0.27 g (32%) of a yellow oil. IR (CH_2Cl_2): 3000–2800, 2020, 1960 cm^{-1}. ^1H NMR (300 MHz, $CDCl_3$): δ 3.73 (d, J(PH) = 12.5 Hz, $P(OMe)_3$), 3.12 (ddd, J(HH) = 17.1 Hz, J(PH) = 7.6 Hz, J(HH) = 2.9 Hz, H–C(4-exo)), 2.82–2.67 (m, H–C(4-endo) and H–C(7-exo)), 2.48 (sept, J(HH) = 2.9 Hz, H–C(5)), 2.27 (t, J(HH) = 5.9 Hz, H–C(7-endo)), 1.90 (d, J(HH) = 9.6 Hz, H–C(1)), 1.72 (m, H–C(8)), 1.50 (m, H–C(8)), 1.47 (s, CH_3), 1.04 (s, CH_3). ^{13}C NMR (50 MHz, $CDCl_3$): δ 199.2 (d, J(PC) = 18 Hz, CO), 194.5 (d, J(PC) = 2 Hz, CO), 139.3 (d, J(PC) = 4 Hz, C(3)), 107.9 (d, J(PC) = 4 Hz, C(2)), 51.4 (s, $P(OMe)_3$), 43.4 (s, C(1) or C(5)), 42.1 (s, C(5) or C(1)), 39.7 (d, J(PC) = 5 Hz, C(6)), 36.0 (d, J(PC) = 4 Hz, CH_2), 32.7 (s, CH_2), 32.3 (d, J(PC) = 4 Hz, CH_2), 27.0 (s, CH_3), 21.4 (s, CH_3). ^{31}P NMR (80.7 MHz, $CDCl_3$): δ 162.1 (s). For optical rotation and CD data, see Table I.

(+)-Tetracarbonyl((+)-neomenthyldiphenylphosphine)-ruthenium ((+)-15). This mononuclear complex was synthesized according to the procedure of Johnson et al.[25] A suspension of 1 g (1.56 mmol) of $Ru_3(CO)_{12}$ in 200 mL hexane was saturated with ethylene and then irradiated with a high-pressure Hg lamp. During irradiation ethylene was bubbled through the solution and a saturated $NaNO_2$ solution was used as a cutoff filter. After approximately 1 h the orange suspension turned into a pale yellow, clear solution of the $Ru(CO)_4(\eta^2$-ethylene) complex. A 4.5 mmol amount (0.5 g) of (+)-NMDPP was added and irradiation carried on until no C_2H_4 development was observed anymore. The solvent was removed in vacuo at room temperature and the oily residue then chromatographed with 4:1 hexane/Et_2O as eluent. The desired product was obtained as orange crystals (0.97 g, 40% based on Ru atoms). Mp: 50 °C. IR (CH_2Cl_2): 2060, 2030, 1980, 1940 cm^{-1}. ^1H NMR (300 MHz, $CDCl_3$): 7.92–7.25 (m, phenyl H), 3.00 (m, H–C(2)), 2.35–1.71 (m, ring H), 1.20 (m, ring H), 1.08 (d, J(HH) = 7.1 Hz, CH_3), 0.90 (m, ring H), 0.78 (d, J(HH) = 6.6 Hz, CH_3), 0.49 (d, J(HH) = 6.8 Hz, CH_3). ^{13}C NMR (50 MHz, $CDCl_3$): δ 226.5 (s, CO), 205.0 (d, J(PC) = 4 Hz, CO), 138.5–128.0 (m, phenyl C), 40.5 (d, J(PC) = 22 Hz, C(1)), 39.3 (d, J(PC) = 2 Hz, CH), 30.8 (d, J(PC) = 6 Hz, CH_2), 30.0 (d, J(PC) = 4 Hz, CH), 28.3 (s, CH_2), 28.0 (d, J(PC) = 8 Hz, CH), 23.9 (s, CH_3), 20.6 (s, CH_3), 17.5 (s, CH_3). ^{31}P NMR (80.7 MHz, $CDCl_3$): δ 48.6 (s).

(–)-(*pR*)-Dicarbonyl[O-4-η-((*E*)-4-phenylbut-3-en-2-one)]((+)-neomenthyldiphenylphosphine)ruthenium ((–)-16a). A mixture of 0.6 g (1.11 mmol) of tetracarbonyl((+)-NMDPP)ruthenium ((+)-**15**) and 0.49 g (3.33 mmol) of (*E*)-4-phenylbut-3-en-2-one in 150 mL of benzene was irradiated with a high-pressure Hg lamp for 24 h. One more portion of the organic ligand was added after 2, 4, 8, and 16 h. After completion of the reaction, no starting material could be detected with TLC. The solvent was removed under vacuum at 40 °C. Excess ligand was removed by distillation (bp 80 °C, 10^{-2} mmHg). The two diastereomers (–)-**16a** and (+)-**16b** could easily be separated by chromatography using 3:1 hexane/Et_2O as eluent. A 0.25-g amount (35%) of (–)-**16a** was obtained as yellow crystals. IR (CH_2Cl_2): 3000–2850, 2010, 1945 cm^{-1}. ^1H NMR (300 MHz, $CHCl_3$): δ 7.40–6.76 (m, phenyl H), 5.60 (dd, J(HH) = 8.0 Hz, J(PH) = 3.6 Hz, H–C(3)), 3.26 (m, H–C(1′)), 2.61 (d, J(PH) = 3.8 Hz, H–C(1)), 2.25–2.16 (m, H–C(3′), H–C(5′) and H–C(7′)), 2.06 (t, J(HH) = J(PH) = 7.8 Hz, H–C(4)), 1.81–1.76 (m, H–C(4′) and H–C(6′)), 1.29 (m, H–C(1′)), 1.20 (d, J(HH) = 7.1 Hz, CH_3), 0.75 (d, J(HH) = 6.6 Hz, CH_3), 0.52 (d, J(HH) = 5.7 Hz, CH_3). ^{13}C NMR (50 MHz, $CHCl_3$): δ 201.7 (d, J(PC) = 9 Hz, CO), 197.6

Table III. Crystallographic Details for (–)-3 and (–)-7

	(–)-3	(–)-7
molecular formula	$C_{15}H_{19}FeO_6P$	$C_{24}H_{37}FeO_3P$
fw	382.12	460.37
mp, °C	60	76
cryst color, habit	red-orange, prism	
cryst size, mm	0.30 × 0.37 × 0.50	0.18 × 0.28 × 0.47
cryst system	orthorhombic	
space group	$P2_12_12_1$	
a, Å	15.165 (1)	12.036 (1)
b, Å	15.558 (2)	24.087 (2)
c, Å	7.174 (2)	8.609 (1)
V, Å^3	1692.5 (4)	2496.0 (4)
Z	4	4
D_{calcd}, Mg m^{-3}	1.500	1.225
μ(Mo Kα), cm^{-1}	10.07	6.85
F(000)	792	984
temp, K	173 ± 1	
scan type	ω–2θ	
ω scan width, deg	1.40 + 0.35 tan θ	1.16 + 0.35 tan θ
2θ limits, deg	5–60 for hkl; 5–45 for $\bar{h}k\bar{l}$	
no. of reflns for cell	25	20
2θ limits for cell, deg	44–47	29–41
no. of reflns collcd	4330	6271
no. of unique reflns	3828	5683
R_{merge} (Friedel pairs not averaged)	0.010	0.012
no. of obsd reflns [$I > 3\sigma(I)$]	3593	4852
weighting, g	0.005	0.005
R	0.0239	0.0273
R_w	0.0247	0.0244
GoF	1.967	1.280
no. of refined params	285	410
N_o/N_v	12.6	11.8
max Δ/σ	0.0003	0.003
max and min Δ, e Å^{-3}	0.42, –0.29	0.29, –0.20

(25) Johnson, B. F. G.; Lewis, J.; Twigg, M. V. *J. Organomet. Chem.* **1974**, *67*, C75.

Table IV. Fractional Atomic Coordinates and Equivalent Isotropic Temperature Factors for (−)-3 and (−)-7

	x	y	z	B_{eq}[a]/B_{iso}, Å^2		x	y	z	B_{eq}[a]/B_{iso}, Å^2
				(−)-3					
Fe	0.09716 (2)	0.21426 (2)	0.78820 (4)	1.55 (1)	C(14)	−0.0614 (2)	0.4036 (1)	0.7633 (4)	2.9 (1)
P	−0.04439 (3)	0.23511 (3)	0.75610 (7)	1.71 (2)	C(15)	−0.1651 (2)	0.2434 (2)	0.4889 (5)	3.6 (1)
O(1)	0.0923 (1)	0.10119 (8)	0.9285 (2)	2.22 (4)	H(3)	0.233 (1)	0.246 (1)	1.021 (3)	2.0 (4)
O(2)	0.1377 (1)	0.1221 (1)	0.4403 (2)	3.20 (8)	H(4)	0.050 (1)	0.215 (1)	1.117 (3)	1.8 (4)
O(3)	0.1552 (1)	0.3752 (1)	0.6222 (2)	2.82 (7)	H(6)	0.212 (1)	0.390 (1)	1.045 (3)	1.8 (5)
O(4)	−0.10950 (9)	0.17148 (8)	0.8642 (2)	2.22 (6)	H(7)	0.193 (1)	0.532 (2)	1.123 (3)	2.7 (5)
O(5)	−0.09103 (9)	0.32084 (8)	0.8319 (2)	2.27 (6)	H(8)	0.059 (1)	0.583 (1)	1.241 (4)	3.9 (5)
O(6)	−0.07382 (9)	0.22983 (9)	0.5415 (2)	2.34 (6)	H(9)	−0.047 (2)	0.479 (2)	1.299 (4)	3.9 (6)
C(1)	0.2516 (2)	0.0777 (2)	0.9026 (4)	2.9 (1)	H(10)	−0.036 (1)	0.334 (1)	1.235 (3)	2.3 (4)
C(2)	0.1727 (1)	0.1323 (1)	0.9484 (3)	2.06 (8)	H(11)	0.307 (2)	0.110 (2)	0.908 (4)	4.0 (6)
C(3)	0.1779 (1)	0.2166 (1)	1.0200 (3)	2.03 (8)	H(12)	0.259 (2)	0.039 (2)	0.994 (3)	3.9 (6)
C(4)	0.0959 (2)	0.2571 (1)	1.0695 (3)	2.00 (8)	H(13)	0.244 (2)	0.048 (1)	0.775 (4)	4.4 (6)
C(5)	0.0898 (2)	0.3479 (1)	1.1253 (3)	2.09 (8)	H(131)	−0.048 (2)	0.065 (2)	0.829 (4)	5.3 (7)
C(6)	0.1578 (2)	0.4076 (2)	1.0932 (3)	2.6 (1)	H(132)	−0.144 (2)	0.049 (2)	0.920 (5)	8. (1)
C(7)	0.1472 (2)	0.4937 (2)	1.1429 (4)	3.2 (1)	H(133)	−0.138 (2)	0.071 (2)	0.718 (5)	6.1 (8)
C(8)	0.0688 (2)	0.5221 (2)	1.2223 (4)	3.3 (1)	H(141)	−0.107 (2)	0.448 (2)	0.806 (4)	5.1 (6)
C(9)	0.0020 (2)	0.4638 (2)	1.2564 (4)	3.2 (1)	H(142)	−0.052 (2)	0.404 (2)	0.634 (4)	5.4 (8)
C(10)	0.0121 (2)	0.3779 (2)	1.2103 (3)	2.7 (1)	H(143)	−0.005 (2)	0.415 (2)	0.835 (4)	5.4 (7)
C(11)	0.1217 (1)	0.1588 (1)	0.5739 (3)	2.03 (8)	H(151)	−0.165 (2)	0.226 (2)	0.347 (4)	6.2 (8)
C(12)	0.1309 (1)	0.3118 (1)	0.6879 (3)	1.91 (8)	H(152)	−0.203 (2)	0.214 (2)	0.564 (4)	4.3 (6)
C(13)	−0.1047 (2)	0.0803 (1)	0.8160 (4)	2.8 (1)	H(153)	−0.176 (2)	0.312 (2)	0.494 (4)	5.4 (7)
				(−)-7					
Fe	0.95121 (2)	0.83514 (1)	0.21951 (3)	1.58 (1)	H(8)	0.886 (2)	1.021 (1)	−0.358 (3)	4.4 (6)
P	1.09084 (4)	0.79957 (2)	0.08031 (6)	1.69 (2)	H(9)	0.882 (2)	0.9294 (9)	−0.447 (3)	3.0 (5)
O(1)	0.8480 (1)	0.76785 (5)	0.2086 (2)	2.15 (6)	H(10)	0.866 (2)	0.8564 (9)	−0.274 (3)	3.3 (5)
O(2)	1.0268 (1)	0.80025 (7)	0.5282 (2)	3.43 (8)	H(11)	0.708 (2)	0.843 (1)	0.454 (3)	4.7 (6)
O(3)	1.0463 (1)	0.94492 (5)	0.2645 (2)	3.44 (7)	H(12)	0.776 (2)	0.7812 (9)	0.491 (3)	3.3 (5)
C(1)	0.7285 (2)	0.8045 (1)	0.4159 (3)	2.9 (1)	H(13)	0.663 (2)	0.787 (1)	0.403 (3)	4.8 (7)
C(2)	0.7913 (2)	0.81010 (8)	0.2646 (3)	2.03 (8)	H(131)	1.114 (2)	0.7206 (9)	−0.066 (3)	3.6 (6)
C(3)	0.7906 (2)	0.85873 (9)	0.1723 (3)	1.92 (8)	H(132)	0.983 (2)	0.7315 (9)	−0.039 (3)	2.9 (5)
C(4)	0.8477 (2)	0.85517 (8)	0.0269 (2)	1.85 (8)	H(141)	1.009 (2)	0.6932 (8)	0.221 (2)	2.4 (4)
C(5)	0.8577 (2)	0.90312 (9)	−0.0789 (3)	2.02 (8)	H(142)	1.131 (2)	0.6789 (7)	0.182 (2)	2.1 (5)
C(6)	0.8545 (2)	0.95833 (9)	−0.0272 (3)	2.4 (1)	H(151)	0.940 (2)	0.631 (1)	0.025 (3)	4.5 (6)
C(7)	0.8616 (2)	1.0020 (1)	−0.1317 (3)	3.2 (1)	H(152)	1.068 (2)	0.621 (1)	−0.027 (3)	5.0 (6)
C(8)	0.8736 (2)	0.9920 (1)	−0.2890 (4)	3.7 (1)	H(161)	0.986 (2)	0.585 (1)	0.274 (4)	5.6 (7)
C(9)	0.8762 (2)	0.9379 (1)	−0.3426 (3)	3.5 (1)	H(162)	1.006 (2)	0.543 (1)	0.128 (3)	6.3 (7)
C(10)	0.8681 (2)	0.8940 (1)	−0.2385 (3)	2.7 (1)	H(163)	1.109 (3)	0.576 (1)	0.207 (4)	7.7 (9)
C(11)	0.9985 (2)	0.81453 (8)	0.4072 (3)	2.14 (8)	H(171)	1.067 (2)	0.8229 (8)	−0.175 (2)	2.8 (5)
C(12)	1.0090 (2)	0.90123 (8)	0.2439 (2)	2.11 (8)	H(172)	1.196 (2)	0.8124 (9)	−0.144 (3)	3.6 (6)
C(13)	1.0591 (2)	0.72898 (8)	0.0131 (3)	2.17 (8)	H(181)	1.214 (2)	0.9048 (9)	−0.036 (3)	2.9 (5)
C(14)	1.0576 (2)	0.68294 (8)	0.1349 (3)	2.45 (9)	H(182)	1.091 (2)	0.9159 (9)	−0.075 (3)	3.3 (5)
C(15)	1.0216 (2)	0.6275 (1)	0.0653 (3)	3.3 (1)	H(191)	1.128 (2)	0.901 (1)	−0.354 (3)	4.8 (7)
C(16)	1.0336 (3)	0.5785 (1)	0.1743 (4)	4.4 (1)	H(192)	1.259 (2)	0.894 (1)	−0.291 (3)	5.5 (7)
C(17)	1.1318 (2)	0.83171 (9)	−0.1046 (3)	2.28 (9)	H(201)	1.139 (2)	0.998 (1)	−0.248 (3)	5.4 (7)
C(18)	1.1559 (2)	0.89403 (9)	−0.1082 (3)	2.4 (1)	H(202)	1.273 (2)	0.988 (1)	−0.215 (4)	5.4 (7)
C(19)	1.1879 (2)	0.9135 (1)	−0.2708 (3)	3.4 (1)	H(203)	1.222 (3)	0.987 (1)	−0.388 (4)	8.5 (9)
C(20)	1.2083 (3)	0.9758 (1)	−0.2813 (5)	4.7 (2)	H(211)	1.205 (2)	0.7634 (8)	0.266 (3)	2.5 (5)
C(21)	1.2223 (2)	0.79003 (9)	0.1854 (3)	2.2 (1)	H(212)	1.273 (2)	0.7730 (9)	0.117 (3)	3.4 (6)
C(22)	1.2745 (2)	0.84175 (9)	0.2569 (3)	2.5 (1)	H(221)	1.220 (2)	0.8644 (9)	0.312 (3)	3.5 (5)
C(23)	1.3758 (2)	0.8290 (1)	0.3570 (3)	2.9 (1)	H(222)	1.291 (2)	0.869 (1)	0.173 (3)	4.7 (6)
C(24)	1.4379 (2)	0.8808 (1)	0.4056 (4)	3.8 (1)	H(231)	1.348 (2)	0.811 (1)	0.444 (3)	3.6 (6)
H(3)	0.761 (1)	0.8910 (7)	0.212 (2)	1.5 (4)	H(232)	1.422 (2)	0.8021 (9)	0.310 (3)	3.4 (5)
H(4)	0.842 (2)	0.8203 (8)	−0.027 (2)	1.9 (4)	H(241)	1.387 (2)	0.910 (1)	0.448 (3)	4.5 (6)
H(6)	0.846 (2)	0.9666 (8)	0.083 (3)	2.0 (4)	H(242)	1.465 (2)	0.899 (1)	0.309 (4)	7.0 (8)
H(7)	0.860 (2)	1.0391 (9)	−0.098 (3)	2.8 (5)	H(243)	1.499 (2)	0.873 (1)	0.482 (3)	6.2 (8)

[a] B_{eq} is defined as one-third of the trace of the orthogonalized $\mathbf{B}_{ij}$ tensor.

(s, CO), 143.1–124.2 (m, C(2) and phenyl C), 80.3 (s, C(3)), 56.6 (s, C(4)), 39.5 (s, CH), 39.0 (d, J(PC) = 19 Hz, CH), 30.9 (s, CH_2), 29.8 (d, J(PC) = 6 Hz, CH), 28.2 (s, CH_2), 27.7 (d, J(PC) = 9 Hz, CH), 24.1 (s, C(1)), 21.4 (s, CH_3), 21.0 (d, J(PC) = 11 Hz, CH_2), 20.6 (s, CH_3), 17.7 (s, CH_3). ^{31}P NMR (80.7 MHz, $CDCl_3$): δ 42.7 (s, br). For optical rotation and CD data, see Table I.

(+)-(*pS*)-Dicarbonyl[O-4-η-((*E*)-4-phenylbut-3-en-2-one)](+)-neomenthyldiphenylphosphine)ruthenium ((+)-16b). The procedure is the same as for (−)-**16a**. This diastereomer was obtained by chromatography as described above as a yellow oil in a yield of 0.234 g (30%). IR (CH_2Cl_2): 3000–2850, 2010, 1945 cm^{-1}. ^{1}H NMR (300 MHz, $CDCl_3$): δ 7.74–6.65 (m, phenyl H), 5.51 (dd, J(HH) = 7.9 Hz, J(PH) = 3.5 Hz, H–C(3)), 3.19–3.08 (m, H–C(1′)), 2.56 (d, J(PH) = 3.8 Hz, H–C(1)), 2.18 (t, J(HH) = J(PH) = 7.9 Hz, H–C(4)), 2.13–0.80 (m, ring H), 1.17 (d, J(HH) = 7.1 Hz, CH_3), 0.71 (d, J(HH) = 6.7 Hz, CH_3), 0.30 (d, J(HH) = 6.8 Hz, CH_3). ^{13}C NMR (50 MHz, $CDCl_3$): δ 201.7 (d, J(PC) = 10 Hz, CO), 197.5 (s, CO), 124.2–143.2 (m, C(2) and phenyl C), 80.5 (s, C(3)), 56.0 (s, C(4)), 39.3 (d, J(PC) = 4 Hz, CH), 37.2 (d, J(PC) = 20 Hz, C(1′)), 30.5 (m, CH_2 and CH), 28.2 (s, CH_2), 27.8 (d, J(PC) = 8 Hz, CH), 23.7 (s, C(1)), 21.3 (d, J(PC) = 2 Hz, CH_3), 20.4 (d, J(PC) = 11 Hz, C(6′)), 17.7 (s, CH_3). ^{31}P NMR (80.7 MHz, $CDCl_3$): δ 42.2 (s). For optical rotation and CD data, see Table I.

Crystallographic Analysis of (−)-3 and (−)-7. Suitable red-orange crystals formed in hexane. Intensity data were collected at low temperature on a Rigaku AFC5R diffractometer mounted on a 12-kW rotating anode generator, using graphite-monochromated Mo Kα radiation (λ = 0.71069 Å). The ω–2θ scan technique was employed with a fixed ω scan speed of 16° min^{-1}. The weak reflections [$I < 10\sigma(I)$] were rescanned up to a maximum of 4 scans, and the counts were accumulated. Stationary background counts were recorded on each side of the reflection with a peak/background counting time ratio of 2:1. The intensities

Table V. Selected Interatomic Distances (Å) and Bond Angles (deg) with Esd's in Parentheses

		(−)-**3**	
Fe–P	2.1831 (5)	P–Fe–O(1)	98.37 (5)
Fe–O(1)	2.028 (1)	P–Fe–C(2)	134.12 (6)
Fe–C(2)	2.064 (2)	P–Fe–C(3)	131.69 (6)
Fe–C(3)	2.065 (2)	P–Fe–C(4)	92.58 (6)
Fe–C(4)	2.125 (2)	P–Fe–C(11)	100.62 (7)
Fe–C(11)	1.802 (2)	P–Fe–C(12)	96.60 (6)
Fe–C(12)	1.756 (2)	O(1)–Fe–C(4)	78.48 (7)
O(1)–C(2)	1.319 (2)	O(1)–Fe–C(11)	90.87 (8)
C(2)–C(3)	1.411 (3)	O(1)–Fe–C(12)	164.51 (8)
C(3)–C(4)	1.438 (3)	C(4)–Fe–C(11)	164.16 (8)
O(2)–C(11)	1.142 (3)	C(4)–Fe–C(12)	96.93 (9)
O(3)–C(12)	1.154 (2)	C(11)–Fe–C(12)	90.26 (9)
		(−)-**7**	
Fe–P	2.2349 (6)	P–Fe–O(1)	97.37 (4)
Fe–O(1)	2.044 (1)	P–Fe–C(2)	133.89 (6)
Fe–C(2)	2.054 (2)	P–Fe–C(3)	135.01 (6)
Fe–C(3)	2.055 (2)	P–Fe–C(4)	96.27 (6)
Fe–C(4)	2.129 (2)	P–Fe–C(11)	98.00 (7)
Fe–C(11)	1.784 (2)	P–Fe–C(12)	96.56 (6)
Fe–C(12)	1.750 (2)	O(1)–Fe–C(4)	77.77 (7)
O(1)–C(2)	1.317 (2)	O(1)–Fe–C(11)	90.85 (8)
C(2)–C(3)	1.415 (3)	O(1)–Fe–C(12)	165.55 (7)
C(3)–C(4)	1.431 (3)	C(4)–Fe–C(11)	162.78 (9)
O(2)–C(11)	1.149 (2)	C(4)–Fe–C(12)	96.89 (9)
O(3)–C(12)	1.158 (2)	C(11)–Fe–C(12)	91.01 (9)

of three representative reflections measured after every 150 reflections showed no decay. Friedel equivalent reflections were recorded for all reflections having $2\theta < 45°$. The data were corrected for Lorentz and polarization effects. An empirical absorption correction was applied[26] (minimum and maximum corrections 0.887 and 1.112 for (−)-**3** and 0.920 and 1.084 for (−)-**7**).

For each structure, the Fe atom was located by the Patterson method,[27] and all remaining non-hydrogen atoms were located in a Fourier expansion of the Patterson solution. The non-hydrogen atoms were refined anisotropically. All of the hydrogen atoms were located in a difference Fourier synthesis, and their positions were allowed to refine together with individual isotropic temperature factors. The structures were refined, on F, by full-matrix least-squares procedures[28] to minimize $\sum w(|F_o| - |F_c|)^2$, where $w^{-1} = \sigma^2(F) + (gF)^2$. A correction for secondary extinction was applied in the case of (−)-**3** only. Plots of $\sum w(|F_o| - |F_c|)^2$ versus $|F_o|$, reflection order in data collection, $(\sin\theta)/\lambda$, and various classes of indices showed no unusual trends. The final difference Fourier maps were essentially featureless with the maximum peaks being in the vicinity of the Fe atom.

Crystal data, data collection, and least-squares parameters are listed in Table III. Neutral-atom scattering factors for non-hydrogen atoms were taken from Cromer and Waber,[29] and the scattering factors for hydrogen atoms were taken from Stewart, Davidson, and Simpson.[30] Anomalous dispersion effects were included in F_c;[31] the values for $\Delta f'$ and $\Delta f''$ were those of Cromer.[32] All calculations were performed using the TEXSAN[12] crystallographic software package, CRYSTALS[13] and SHELXS86,[27] on a Vax 6320 computer. Final atomic coordinates and selected bond lengths and angles are presented in Tables IV and V, respectively.

Acknowledgment. This work was supported by the Swiss National Science Foundation.

Supplementary Material Available: Tables of bond lengths and angles, anisotropic thermal parameters, and torsion angles (4 pages). Ordering information is given on any current masthead page.

OM920375W

(26) Walker, N.; Stuart, D. *Acta Crystallogr., Sect. A* **1983**, *39*, 158.
(27) Sheldrick, G. M. SHELXS86. A program for crystal structure solution. *In Crystallographic Computing 3*; Sheldrick, G. M., Krüger, C., Goddard, R. Eds; Oxford University Press: Oxford, U.K., 1985; pp 175–189.
(28) Busing, W. R.; Martin, K. O.; Levy, H. A., ORFLS. A FORTRAN crystallographic least squares program. Report ORNL-TM-305, Oak Ridge National Laboratory, Oak Ridge, TN, 1962.
(29) Cromer, D. T.; Waber, J. T. *International Tables for X-ray Crystallography*; The Kynoch Press: Birmingham, England (present distributor Kluwer Academic Publishers, Dordrecht, The Netherlands), 1974; Vol. IV, Table 2.2A, pp 71–98.
(30) Stewart, R. F.; Davidson, E. R.; Simpson, W. T. *J. Chem. Phys.* **1965**, *42*, 3175.
(31) Ibers, J. A.; Hamilton, W. C. *Acta Crystallogr.* **1964**, *17*, 781.
(32) Cromer, D. T.; Waber J. T. *International Tables for X-ray Crystallography*, Vol. IV, The Kynoch Press: Birmingham, England (present distributor Kluwer Academic Publishers, Dordrecht, The Netherlands), 1974; Vol. IV, Table 2.3.1, pp 149–150.